

Article

# Novel Electrochemical Sensors Based on Cuprous Oxide-Electrochemically Reduced Graphene Oxide Nanocomposites Modified Electrode toward Sensitive Detection of Sunset Yellow

Quanguo He <sup>1,2,†</sup>, Jun Liu <sup>1,2,†</sup>, Xiaopeng Liu <sup>2</sup>, Yonghui Xia <sup>3</sup>, Guangli Li <sup>1,2,\*</sup>, Peihong Deng <sup>4</sup> and Dongchu Chen <sup>1,\*</sup>

<sup>1</sup> School of Materials Science and Energy Engineering, Foshan University, Foshan 528000, China; hequanguo@126.com (Q.H.); liu.jun.1015@163.com (J.L.)

<sup>2</sup> College of Life Sciences and Chemistry, Hunan University of Technology, Zhuzhou 412007, China; amitu0321@163.com

<sup>3</sup> Zhuzhou Institute for Food and Drug Control, Zhuzhou 412000, China; sunnyxia0710@163.com

<sup>4</sup> Department of Chemistry and Material Science, Hengyang Normal University, Hengyang 421008, China; dph1975@163.com

\* Correspondence: guangli010@hut.edu.cn (G.L.); chendc@fosu.edu.cn (D.C.); Tel./Fax: +86-731-22183382 (G.L. & D.C.)

† These authors contributed equally to this work.

Received: 30 July 2018; Accepted: 21 August 2018; Published: 24 August 2018



**Abstract:** Control and detection of sunset yellow is an utmost demanding issue, due to the presence of potential risks for human health if excessively consumed or added. Herein, cuprous oxide-electrochemically reduced graphene nanocomposite modified glassy carbon electrode (Cu<sub>2</sub>O-ErGO/GCE) was developed for the determination of sunset yellow. The Cu<sub>2</sub>O-ErGO/GCE was fabricated by drop-casting Cu<sub>2</sub>O-GO dispersion on the GCE surface following a potentiostatic reduction of graphene oxide (GO). Scanning electron microscope and X-ray powder diffractometer was used to characterize the morphology and microstructure of the modification materials, such as Cu<sub>2</sub>O nanoparticles and Cu<sub>2</sub>O-ErGO nanocomposites. The electrochemical behavior of sunset yellow on the bare GCE, ErGO/GCE, and Cu<sub>2</sub>O-ErGO/GCE were investigated by cyclic voltammetry and second-derivative linear sweep voltammetry, respectively. The analytical parameters (including pH value, sweep rate, and accumulation parameters) were explored systematically. The results show that the anodic peak currents of Cu<sub>2</sub>O-ErGO/GCE are 25-fold higher than that of the bare GCE, due to the synergistic enhancement effect between Cu<sub>2</sub>O nanoparticles and ErGO sheets. Under the optimum detection conditions, the anodic peak currents are well linear to the concentrations of sunset yellow, ranging from  $2.0 \times 10^{-8}$  mol/L to  $2.0 \times 10^{-5}$  mol/L and from  $2.0 \times 10^{-5}$  mol/L to  $1.0 \times 10^{-4}$  mol/L with a low limit of detection (S/N = 3,  $6.0 \times 10^{-9}$  mol/L). Moreover, Cu<sub>2</sub>O-ErGO/GCE was successfully used for the determination of sunset yellow in beverages and food with good recovery. This proposed Cu<sub>2</sub>O-ErGO/GCE has an attractive prospect applications on the determination of sunset yellow in diverse real samples.

**Keywords:** cuprous oxide nanoparticles; reduced graphene oxide; modified electrode; sunset yellow; second-derivative linear sweep voltammetry

## 1. Introduction

Sunset yellow, as a common azo colorant, has been widely added in several beverages (such as carbonated beverage, orange juice, and Fanta drink) and food (i.e. candies, cakes, cheese) to improve

the appearance and appetite [1,2]. Sunset yellow contains an azo group (-N=N-) and aromatic ring structure, which may cause mutagenic and carcinogenic risk for human [3,4]. As a result, it can bring many serious health problems, such as hepatocellular damage, kidney failures, headache, cancers, and attention deficit hyperactivity disorder (ADHD), when it is excessively consumed [5]. Hence, the additive amount of sunset yellow in beverages and food demands strict control and regulation. European Food Safety Authority (EFSA) recommends an acceptable daily intake (ADI) for sunset yellow of  $1.0 \text{ mg kg}^{-1}$  body weight [6]. In some countries, it was explicitly stated that the permitted maximum content of sunset yellow in nonalcoholic beverages is  $100 \text{ } \mu\text{g mL}^{-1}$  [7]. Moreover, Finland and Norway even has already banned the use of sunset yellow in foods [6]. While considering the food quality and safety, it is urgent to develop reliable analytical techniques for the quick detection of this food dye.

At present, various techniques have been developed for sunset yellow, including high performance liquid chromatography (HPLC) [8], thin layer chromatography [9], spectrophotometry [10], fluorometry [11], and capillary electrophoresis [12]. Although these methods have been proved to be reliable, they still have some disadvantages, such as time-consuming, complicated preprocessing, and expensive equipment. Recently, electrochemical analysis has been widely used for the detection of bioactive molecules, nutrients, food additives, as well as contaminants, due to its considerable merits such as low cost, simple operation, rapid response, high sensitivity and sensitivity. As we all know, the key issue for electrochemical detection toward sunset yellow is to develop ultrasensitive modified electrodes.

Nanostructure precious metals or alloys have become the preferred electrode modification materials for the sensitive detection of sunset yellow, due to their superior electrocatalytic activity [7,13–17]. For example, Wang and coworkers developed a promising electrochemical sensor based on Au-Pd and reduced graphene oxide nanocomposite decorated electrode (Au-Pd-RGO/GCE) [17]. The Au-Pd-RGO/GCE exhibited good stability, superior electrocatalytic performance, low detection limit ( $1.5 \text{ nmol/L}$ ), and wide response range ( $0.686\text{--}331.686 \text{ } \mu\text{mol/L}$ ). Pd-Ru nanoparticles incorporated carbon aerogel nanocomposites (Pd-Ru/CA) have been successfully used for electrochemical detection and catalytic degradation of sunset yellow [16]. The Pd-Ru/CA nanocomposite decorated screen printed carbon electrode (Pd-Ru/CA/SPCE) showed a low detection limit ( $7.1 \text{ nmol/L}$ ) and high sensitivity ( $3.571 \text{ } \mu\text{A}/(\text{ } \mu\text{mol/L cm}^2)$ ). Electrochemical sensing platform based on Au NPs and reduced graphene modified GCE (Au NPs/RGO/GCE) was constructed for the quantitative analysis of sunset yellow, and the Au NPs/RGO/GCE had excellent catalytic activity toward the oxidation of sunset yellow [15]. The proposed electrode showed wide linear response range of  $0.002\text{--}109.14 \text{ } \mu\text{mol/L}$  and low detection limit of  $2 \text{ nmo/L}$  ( $S/N = 3$ ). Au NPs decorated carbon-paste electrode (Au NPs/CPE) was also fabricated for the simultaneous detection sunset yellow and Tartrazine [7]. The Au NPs/CPE displayed low detection limits of  $3.0 \times 10^{-8}$  and  $2.0 \times 10^{-9} \text{ mol/L}$  for sunset yellow and Tartrazine, respectively. These precious metals-based modified electrodes can detect sunset yellow at the nanomole level; however, the scarcity and high cost of precious metals or alloys have seriously hindered the broad practical applications.

When compared to precious metals or alloys, transition metals and metal oxides have outstanding advantages in terms of abundance and cost. What is more, transition metals and metal oxides also have excellent catalytic activity. In our previous work,  $\text{Cu}_2\text{O-RGO}$  nanocomposite [18],  $\text{NH}_2\text{-Fe}_3\text{O}_4\text{-RGO}$  nanocomposite [19],  $\text{MnO}_2\text{-RGO}$  nanocomposite [20],  $\text{TiO}_2\text{-RGO}$  nanocomposite [21], and  $\alpha\text{-MnO}_2\text{/N-doped ketjenblack carbon composite}$  [22,23] demonstrated excellent electrochemical sensing performance toward the detection of dopamine and Tartrazine and superior electrocatalytic activity in oxygen reduction reaction (ORR) & oxygen evolution reaction (OER). Recently, few researchers have devoted to developing transition metal oxide modified electrodes for the determination of sunset yellow. For example, Dorraji et al. [24] developed ZnO/cysteic acid nanocomposite modified electrode (ZnO/CA/GCE), and successfully used for simultaneous determination of sunset yellow and Tartrazine. The ZnO/CA/GCE exhibited two linear response

ranges in the concentration ranges of 0.1–3.0  $\mu\text{mol/L}$ , and 0.07–1.86  $\mu\text{mol/L}$ , and detection limits of 0.03  $\mu\text{mol/L}$  and 0.01  $\mu\text{mol/L}$  for sunset yellow and Tartrazine, respectively. However, the linear dynamic response range is limited for trace detection of sunset yellow. The detection capacity of sunset yellow has been improved with graphene and mesoporous  $\text{TiO}_2$  composite [25] and  $\text{ZnO/RGO/ZnO@Zn}$  [26] modified electrodes, and they showed superior sensing performance (i.e., linear ranges, detection of limit) that was comparable to precious metal modified electrode. Although some progress has been made, there are only few related reports concerning the transition metal oxide modified electrodes. Therefore, it is still worthwhile to develop novel transition metal oxide modified electrodes for sensitive detection of sunset yellow.

Among transition oxides, cuprous oxide ( $\text{Cu}_2\text{O}$ ) is an environmentally friendly p-type semiconductor material, which has been widely used in solar cells and photo catalysis [27,28], due to its unique electronic structure and excellent catalytic performances. However, its electrical conductivity is poor due to the nature of semiconductor. To resolve this problem,  $\text{Cu}_2\text{O}$  nanoparticles are often composited or hybridized with conductive materials [29–33], to decrease the charge transfer resistance and eventually enhance the electrochemical performance. Graphene, as an emerging two-dimensional (2D) carbon material, has been usually used as conductive materials in modified electrodes, owing to its high specific surface area, excellent electrical conductivity, superior electrochemical performance, and fast heterogeneous electron transfer rate. It has been reported that graphene-based modified electrodes have been widely employed for the determination of azo dyes, such as sunset yellow, Tartrazine, and Amaranth [34–36]. However, to our best knowledge,  $\text{Cu}_2\text{O}$ /reduced graphene oxide nanocomposite modified electrode toward sensitive detection of sunset yellow has not been reported.

Graphene usually prepared from graphene oxide (GO) by electrochemical reduction method in the field of electrochemical analysis. The chemically reduced graphene oxide is hydrophobic, due to the removal of most oxygen-containing functional groups. As a result, the chemically graphene oxide tends to agglomerate resulting in a degradation on sensing performance. The agglomeration issue can be overcome by introducing the surfactants [37], which can effectively improve the dispersibility. However, the electrical conductivity also declined due to the use of surfactants. Electrochemically reduction method is a green and efficient method to obtain reduced graphene oxide that not require any reductants. Moreover, the residual oxygen-containing functional groups can be tuned by facial adjusting the electrochemical parameter, such as reduction potential, reduction time, and scanning cycles [18,19,21]. In other words, the property of reduced graphene oxide can be tailored by electrochemical parameters. For these reasons, the electrochemically reduced graphene oxide (ErGO) have been widely used for constructing diverse sensors.

Inspired by the foregoing reports, herein ErGO was composited with low cost and excellent electrocatalytic activity  $\text{Cu}_2\text{O}$  nanoparticles, aiming to develop a cost-effective, high sensitive, and good selective modification materials to substitute the precious metal-based materials. Meanwhile, the  $\text{Cu}_2\text{O-ErGO}$  nanocomposites are expected to exert their synergistic sensitizing effects to improve the sensing performance. Then,  $\text{Cu}_2\text{O-ErGO}$  nanocomposites was modified on the surface of the glassy carbon electrode (GCE) to construct a novel sensor toward sunset yellow. The  $\text{Cu}_2\text{O-ErGO}$  modified glassy carbon electrode ( $\text{Cu}_2\text{O-ErGO/GCE}$ ) was prepared while using a facile drop-casting technique in combination with electrochemical reduction. The electrochemical behavior of sunset yellow on the  $\text{Cu}_2\text{O-ErGO/GCE}$  were investigated by cyclic voltammetry and second-derivative linear sweep voltammetry. The effect of detection conditions (such as pH value, sweep rate, and accumulation parameters) on the electrochemical response were also explored. Finally, the proposed  $\text{Cu}_2\text{O-ErGO/GCE}$  was used to detect the content of sunset yellow in soda drinks, orange juice, and candies samples while using second-derivative linear sweep voltammetry.

## 2. Results and Discussion

### 2.1. Morphology and Microstructural Characterization

The surface morphologies of  $\text{Cu}_2\text{O}$  nanoparticles ( $\text{Cu}_2\text{O}$  NPs) and  $\text{Cu}_2\text{O}$ -ErGO nanocomposites were characterized by scanning electron microscope (SEM, Hitachi S-3000N, Tokyo, Japan). The SEM images are shown in Figure 1A,B, respectively. The  $\text{Cu}_2\text{O}$  NPs exhibit cubic-like structure with uniform size, and the particle size is estimated to about 150 nm. Obviously, the thin layer ErGO sheets were successfully coated on the surface of  $\text{Cu}_2\text{O}$  nanoparticles. Moreover, the particle size of  $\text{Cu}_2\text{O}$ -ErGO nanocomposite increases slightly, which facilitates the adsorption of sunset yellow. The  $\text{Cu}_2\text{O}$  NPs were further characterized by X-ray diffraction (XRD, JEOL JEM-2010 (HT, Tokyo, Japan) and the XRD pattern of  $\text{Cu}_2\text{O}$  NPs is plotted in Figure 1C. The diffraction peaks of  $\text{Cu}_2\text{O}$  nanoparticles are clearly indexed into the pure cubic phase of  $\text{Cu}_2\text{O}$  (JSPDS78-2076), suggesting that the cubic phase of  $\text{Cu}_2\text{O}$  nanoparticles was prepared.

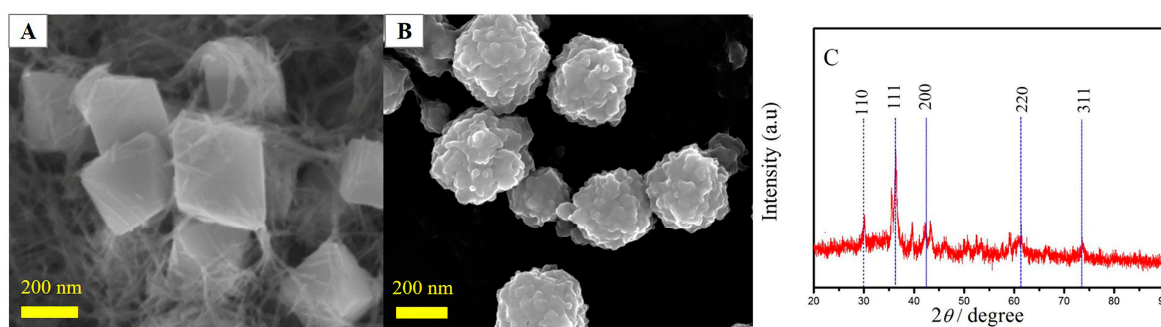


**Figure 1.** The scanning electron microscope (SEM) photos of cuprous oxide ( $\text{Cu}_2\text{O}$ ) nanoparticles (A) and cuprous oxide-electrochemically reduced graphene oxide ( $\text{Cu}_2\text{O}$ -ErGO) nanocomposites (B); and, (C) The X-ray diffraction (XRD) pattern of  $\text{Cu}_2\text{O}$  nanoparticles.

### 2.2. Electrochemical Behavior of Sunset Yellow on Modified Electrodes

Second-derivative linear sweep voltammetric responses of  $1.0 \times 10^{-5}$  mol/L sunset yellow on different electrodes are presented in Figure 2. On the bare GCE, a weak anodic peak of sunset yellow appears at 798 mV with the anodic peak current ( $i_{\text{pa}}$ ) of 0.725  $\mu\text{A}$ . On the GO/GCE, the oxidation peak current of sunset yellow decreases to 0.497  $\mu\text{A}$ , which is mainly due to the present of the poor electrical conductivity of GO. On the  $\text{Cu}_2\text{O}$ -GO/GCE, an apparent anodic peak of occurred at 770 mV, and the  $i_{\text{pa}}$  increases to 0.925  $\mu\text{A}$ , probably owing to the electrocatalytic activity of  $\text{Cu}_2\text{O}$  nanoparticles. When the GO was electrochemically reduced to ErGO, the anodic peak appears at 792 mV and the  $i_{\text{pa}}$  increases to 16.93  $\mu\text{A}$ . This phenomenon may be related to the high electrical conductivity, large specific surface area, and rapid heterogeneous electron transfer rate of ErGO. Moreover, the adsorption capacity of sunset yellow on the electrode surface is improved greatly by the  $\pi$ - $\pi$  interaction, because the conductive carbon-conjugated networks are restored after the reduction process. When the GCE was modified with  $\text{Cu}_2\text{O}$ -ErGO nanocomposites, the  $i_{\text{pa}}$  is the largest (18.08  $\mu\text{A}$ ), which is about 25 fold greater than that of bare GCE. It mainly due to the synergistic enhancement effect between  $\text{Cu}_2\text{O}$  nanoparticles and ErGO sheets, which significantly improves the sensitivity of sunset yellow detection.

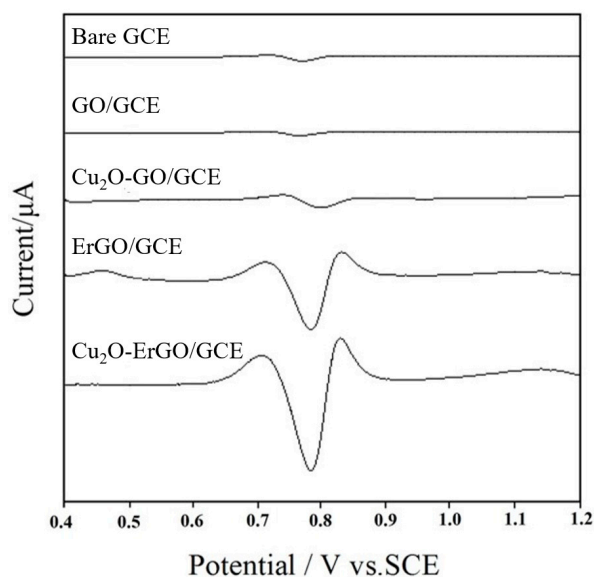


**Figure 2.** Second-derivative linear sweep voltammograms of  $1.0 \times 10^{-5}$  mol/L sunset yellow on the different electrodes.

The electrochemical behavior of  $1.0 \times 10^{-5}$  mol/L sunset yellow on the GCE (a), GO/GCE (b),  $\text{Cu}_2\text{O-GO/GCE}$  (c), ErGO/GCE (d), and  $\text{Cu}_2\text{O-ErGO/GCE}$  (e) were further investigated by cyclic voltammetry (Figure 3). All of the electrodes appear a pair of redox peaks, meaning that sunset yellow undergoes a quasi-reversible process. Obviously, a pair of sharp redox peaks occurs on the ErGO/GCE and  $\text{Cu}_2\text{O-ErGO/GCE}$ . Furthermore, the order of anodic peak currents obtained from cyclic voltammograms is consistent with the second-derivative linear sweep voltammograms, which further confirms that  $\text{Cu}_2\text{O-ErGO}$  nanocomposites can significantly enhance the electrochemical response toward sunset yellow.

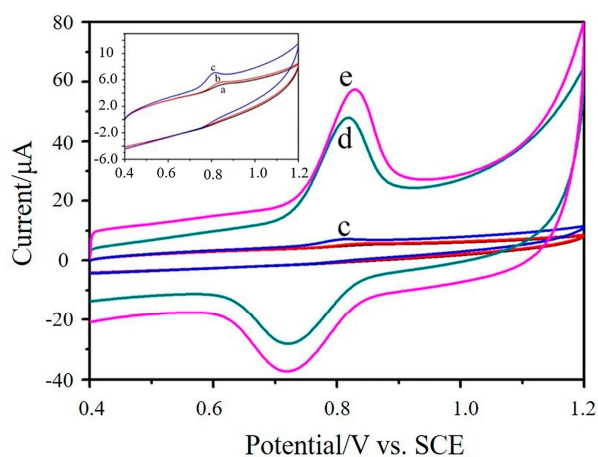


**Figure 3.** Cyclic voltammograms of  $1.0 \times 10^{-5}$  mol/L sunset yellow recorded on the glassy carbon electrode (GCE) (a), graphene oxide/glassy carbon electrode (GO/GCE) (b),  $\text{Cu}_2\text{O-graphene oxide}$  nanocomposite modified glass carbon electrode ( $\text{Cu}_2\text{O-GO/GCE}$ ) (c), electrochemically reduced graphene oxide modified glass carbon electrode (ErGO/GCE) (d) and  $\text{Cu}_2\text{O-ErGO}$  modified glassy carbon electrode ( $\text{Cu}_2\text{O-ErGO/GCE}$ ) (e). The inset is the magnification of the cyclic voltammograms recorded on the GCE (a), GO/GCE (b) and  $\text{Cu}_2\text{O-GO/GCE}$  (c).

### 2.3. Effect of pH Value

Since proton ( $H^+$ ) plays an important role on the redox of sunset yellow, so it is worthwhile investigating the influence of pH value on the response peak current of sunset yellow. The  $i_{pa}$  of sunset yellow recorded in various pH PBS solution are depicted in Figure 4A. The  $i_{pa}$  of sunset yellow increases gradually as the pH value increases. When the pH value increases to 3.8, the largest  $i_{pa}$  is obtained. Afterwards the  $i_{pa}$  decreases slowly with the pH value further increasing. Hence, the pH 3.8 PBS solution was employed as supporting electrolytes on the subsequent experiments. Furthermore, the anodic peak potential ( $E_{pa}$ ) of sunset yellow is negatively shifted with the increase of pH value. As plotted in Figure 4B, there is a good linear relationship between  $E_{pa}$  and pH value, confirming that protons are involved in the oxidation of sunset yellow. The linear regression equation can be expressed as  $E_{pa} (V) = -0.0570 \text{ pH} + 1.0167$  ( $R^2 = 0.998$ ). According to Nernst equation, its slope ( $-0.0570 \text{ V/pH}$ ) approaches to the theoretical value ( $-0.0590 \text{ V/pH}$ ), suggesting that the equal amounts of proton and electron involve in the electrochemical oxidation of sunset yellow [38].

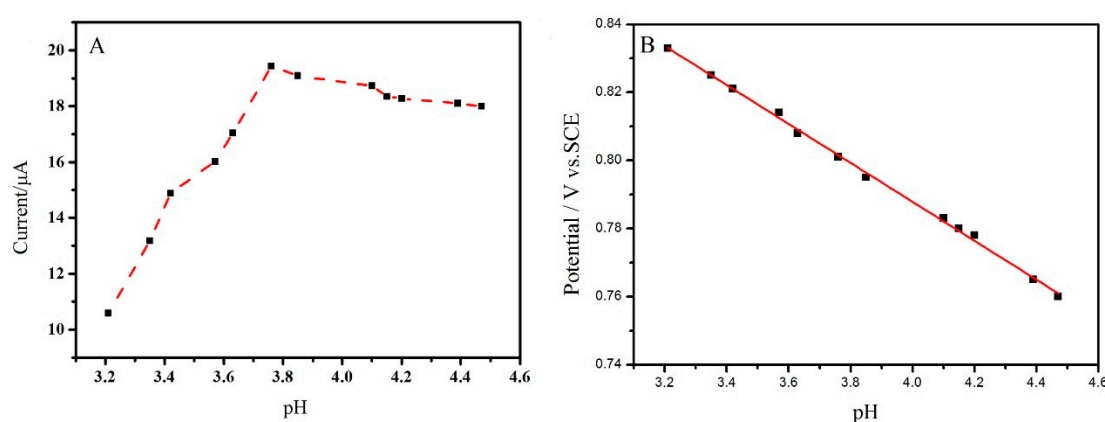


**Figure 4.** (A) Effects of pH value on the anodic peak currents of  $1.0 \times 10^{-5}$  mol/L sunset yellow on the  $\text{Cu}_2\text{O-ErGO/GCE}$ ; and, (B) The plot of the anodic peak potential of  $1.0 \times 10^{-5}$  mol/L sunset yellow against pH value.

### 2.4. Effect of Sweep Rates

Sweep rate is a crucial parameter that directly affects the electrochemical response of analysts on the modified electrodes. Moreover, it is a powerful tool to reveal the electrochemical reaction mechanism. Cyclic voltammograms at various sweep rates were recorded at 0.1 mol/L PBS solution containing  $1 \times 10^{-5}$  mol/L sunset yellow while using the  $\text{Cu}_2\text{O-ErGO/GCE}$ , and their corresponding cyclic voltammograms are shown in the Figure 5A. As expected, with sweep rates increasing, the anodic peaks shift toward positive direction, while the cathodic peaks shift negatively, indicating that the oxidation of sunset yellow on the  $\text{Cu}_2\text{O-ErGO/GCE}$  is quasi-reversible. Both the anodic peak currents ( $i_{pa}$ ) and cathodic peak currents ( $i_{pc}$ ) increase with the sweep speeding up, however, the background currents also increase. To purist high signal-to-noise (S/N), a suitable sweep rate is recommended as 100 mV/s. It can be clearly seen from Figure 5B that both the anodic peak currents ( $i_{pa}$ ) and cathodic peak currents ( $i_{pc}$ ) of sunset yellow is nearly linear with the sweep rates ( $v$ ). Their linear equations are expressed as:  $i_{pa} (\mu\text{A}) = 0.2968 v (\text{mV/s}) - 4.791$  ( $R^2 = 0.998$ ) and  $i_{pc} (\mu\text{A}) = -0.1471 v (\text{mV/s}) + 1.659$  ( $R^2 = 0.997$ ), suggesting that the oxidation of sunset yellow on the  $\text{Cu}_2\text{O-ErGO/GCE}$  is controlled by the adsorption process [39].

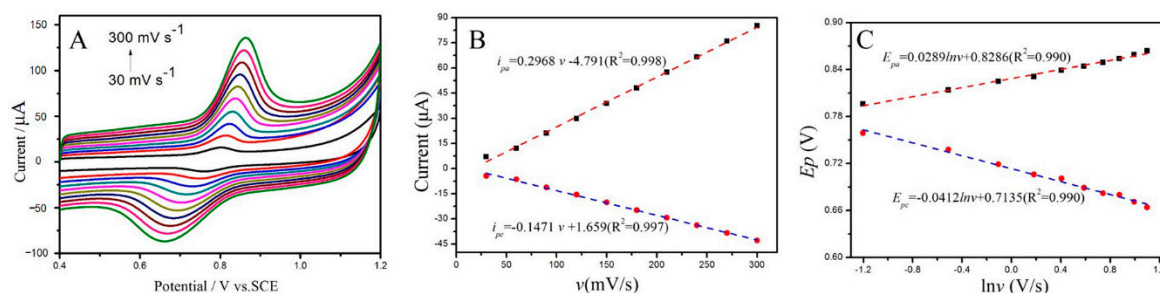


**Figure 5.** (A) Cyclic voltammograms of  $1.0 \times 10^{-5}$  mol/L sunset yellow on the  $\text{Cu}_2\text{O-ErGO/GCE}$  recorded at various sweep rates (30  $\text{mV/s}$ –300  $\text{mV/s}$ ); (B) Linear plots of anodic and cathodic peak currents ( $i_{pa}$  and  $i_{pc}$ ) of sunset yellow against sweep rates ( $v$ ); and (C) Linear plots of anodic and cathodic peak potential ( $E_{pa}$  and  $E_{pc}$ ) of sunset yellow against Napierian Logarithm of sweep rates ( $\ln v$ ). Supporting electrolytes: 0.1 mol/L PBS.

It is observed that both the anodic peak potential ( $E_{pa}$ ) and the cathodic peak potential ( $E_{pc}$ ) is well linear to the Napierian Logarithm of sweep rates ( $\ln v$ ). Their corresponding linear equations are  $E_{pa}$  (V) =  $0.0289\ln v$  (V/s) + 0.8286 ( $R^2 = 0.990$ ) and  $E_{pc}$  (V) =  $-0.0412\ln v$  (V/s) + 0.7135 ( $R^2 = 0.990$ ). As for an adsorption-controlled and quasi-reversible process, according to the Laviron equation [40], the peak potential and the sweep rate follows the following relationship:

$$E_{pa} = E^{0'} + \frac{RT}{(1-\alpha)nF} \left[ 0.78 + \ln\left(\frac{D^{1/2}}{K_s}\right) - \frac{1}{2} \ln \frac{RT}{(1-\alpha)nF} \right] + \frac{RT}{2(1-\alpha)nF} \ln v \quad (1)$$

$$E_{pc} = E^{0'} + \frac{RT}{\alpha nF} \left[ 0.78 + \ln\left(\frac{D^{1/2}}{K_s}\right) - \frac{1}{2} \ln \frac{RT}{\alpha nF} \right] - \frac{RT}{2\alpha nF} \ln v \quad (2)$$

where  $E_{pa}$  (V) and  $E_{pc}$  (V) represents the anodic peak potential and the cathodic peak potential, respectively;  $v$  (V/s) denotes the sweep rate;  $\alpha$  is the charge transfer coefficient;  $k_s$  is the heterogeneous electron transfer rate;  $n$  is the electron transferred number;  $T$  is Kelvin temperature;  $F$  is Faraday constant (96,480 C/mol); and,  $R$  is molar gas constant (8.314 J/(mol·K)). Combining the slopes of Equations (1) and (2) with the  $E_{pa}/E_{pc}$  vs.  $\ln v$  equations, the charge transfer coefficient  $\alpha$  is estimated to be 0.45 and the electron transferred number  $n$  is around 1. Since the equal amount of proton and electron participates in the oxidation process, the electrochemical oxidation of sunset yellow is 1 electron and 1 proton process, which is in accordance with the previous studies [39,41]. Hence, the electrochemical oxidation mechanism of sunset yellow on the  $\text{Cu}_2\text{O-ErGO/GCE}$  can be inferred in Figure 6.

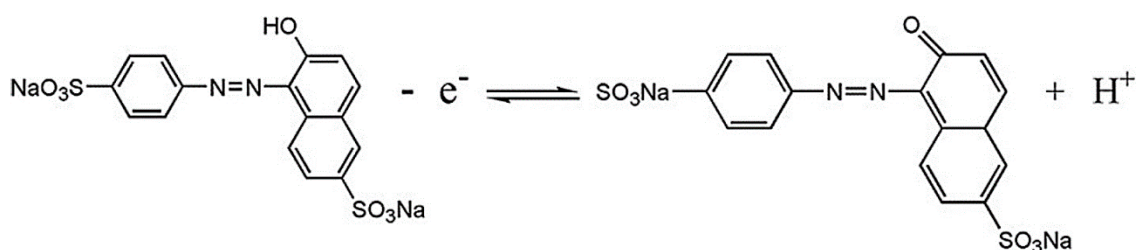


**Figure 6.** The mechanism for the electrochemical processes of sunset yellow on the  $\text{Cu}_2\text{O-ErGO/GCE}$ .

### 2.5. Effect of Accumulation Parameters

Accumulation is a simple and effective technique to improve the electrochemical response. Since the electrochemical oxidation of sunset yellow is an adsorption-controlled process, so accumulation were performed before second-derivative linear sweep voltammetry. As we all know,

accumulation potential as well as time are two important parameters that affect the response peak current greatly, so it is a worthwhile optimization. The  $\text{Cu}_2\text{O-ErGO/GCE}$  was accumulated at different accumulation potential for 240 s firstly. Then, their anodic peak currents ( $i_{\text{pa}}$ ) of sunset yellow were recorded in 0.1 mol/L PBS solution (pH 3.8) while using second-derivative linear sweep voltammetry. The effect of the accumulation potential on the  $i_{\text{pa}}$  of sunset yellow is presented in Figure 7A. The  $i_{\text{pa}}$  increases gradually with the rising of accumulation potential. When the accumulation potential reaches 0.4 V, the strongest  $i_{\text{pa}}$  is obtained. Afterwards, the  $i_{\text{pa}}$  decreases with the accumulation potential further increasing. Therefore, 0.4 V was selected in the subsequent experiments. Furthermore, the influence of accumulation time was also explored. Similarly, the  $\text{Cu}_2\text{O-ErGO/GCE}$  was accumulated at an optimized accumulation potential for various time. Then, their  $i_{\text{pa}}$  of sunset yellow were recorded and compared. As shown in Figure 7B, the  $i_{\text{pa}}$  increases with the prolong of the accumulation during the first 180 s; then  $i_{\text{pa}}$  keep stable with the accumulation time further prolonging, demonstrating that the adsorption of sunset yellow achieved saturated. Hence, 180 s is recommended as the optimum accumulation time.

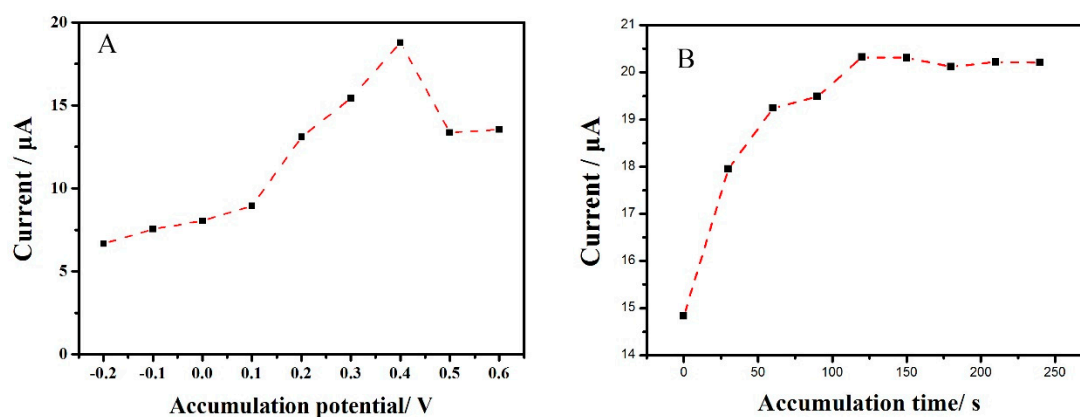


**Figure 7.** Influences of accumulation potential (A), and accumulation time (B) on the anodic peak currents of  $1.0 \times 10^{-5}$  mol/L sunset yellow on the  $\text{Cu}_2\text{O-ErGO/GCE}$ .

## 2.6. Standard Curves, Linear Range and Limit of Detection

With the optimal analytical parameters, the  $i_{\text{pa}}$  of different concentrations of sunset yellow standard solution was determined by second-derivative linear sweep voltammetry. Figure 8A shows the second-derivative linear sweep voltammograms of various concentrations of sunset yellow. There are two linear response ranges for the detection of sunset yellow, namely  $2.0 \times 10^{-8} \sim 2.0 \times 10^{-5}$  mol/L (Figure 8B) and  $2.0 \times 10^{-5}$  mol/L  $\sim 1.0 \times 10^{-4}$  mol/L (Figure 8C). Their corresponding linear equations are  $i_{\text{pa}} (\mu\text{A}) = 1.597c (\mu\text{mol/L}) + 2.628$  ( $R^2 = 0.973$ ) and  $i_{\text{pa}} (\mu\text{A}) = 0.0775c (\mu\text{mol/L}) + 30.36$  ( $R^2 = 0.992$ ), respectively. The limit of detection (LOD,  $S/N = 3$ ) is estimated to be  $6.0 \times 10^{-9}$  mol/L. The linear response range is lower than the permitted maximum content of sunset yellow ( $2.2 \times 10^{-4}$  mol/L), so that the  $\text{Cu}_2\text{O-ErGO/GCE}$  can be applied to detection sunset yellow by a direct or the dilution method. A comparison on sensing performances toward sunset yellow between the existing modified electrodes and  $\text{Cu}_2\text{O-ErGO/GCE}$  is summarized on Table 1.

**Table 1.** Comparison the sensing performances toward the detection of sunset yellow between the existing modified electrodes and the proposed Cu<sub>2</sub>O-ErGO/GCE.

Modified Electrodes	Method	Metrological Parameters	Linear Range (μmol/L)	LOD (μmol/L)	Reference
PLPA/GCE	DPV	0.1 M phosphate-citrate buffer solution (pH 7.0); accumulation for 60 s	0.04–14	0.040	[42]
MIP/f-MWCNTs/GCE	DPV	0.1 M CBS solution (pH 5.0); accumulation for 30 min; scanned at 10 mV/s	0.05–100	0.005	[43]
Au-Pd-RGO/GCE	DPV	0.1 M PBS (pH 4.0); scanned at 50 mV/s	0.69–332	0.0015	[17]
CTAB-Gr-Pt/GCE	DPV	0.1 M PBS (pH 3.0); accumulation for 3 min	0.0085–1.0; 1.0–30	0.0042	[44]
GO/AgNPs-MIPs/GCE	LSV	0.1 M PBS (pH 5.5); accumulation for 7 min; scanned at 50 mV/s	0.1–0.6; 0.6–12	0.02	[45]
ILRGO-Au/GCE	SWV	0.1 M BR buffer solution (pH 7.0); accumulation for 300 s	0.004–1.0	0.00052	[13]
Au NPs/CPE	DPV	0.1 M PBS (pH 4.0); accumulation for 1 min; modulation amplitude = 60 mV and scan rate = 60 mV/s	0.1–2.0	0.03	[7]
MWCNT/GCE	DPV	0.1 M PBS (pH 7.0); accumulation at open circuit potential for 2 min; potential increment of 0.004 V, pulse amplitude of 0.05 V, and pulse period of 0.2 s	0.55–7.0	0.12	[46]
PDDA-Gr-Pd/GCE	DPV	0.1 M PBS (pH 3.0); accumulation for 5 min	0.01–10	0.002	[47]
Fe <sub>3</sub> O <sub>4</sub> @SiO <sub>2</sub> -NPs@MIP/Gr/GCE	DPV	0.1 M PBS (pH 8.0); pulse amplitude = 0.05 V; pulse interval time = 0.05 s, and scan rate = 0.02 V/s for differential pulse voltammetry	0.02–20	0.0055	[48]
Cu <sub>2</sub> O-ErGO/GCE	SDLSV	0.1 M PBS (pH 3.8); accumulation at 0.4 V for 180 s; scanned at 100 mV/s	0.02–20; 20–100	0.006	This work

The linear ranges and LOD of the proposed Cu<sub>2</sub>O-ErGO/GCE are at least comparable to and even better than most of the previous reports. Moreover, Cu<sub>2</sub>O-ErGO/GCE have outstanding advantages over noble metal modified electrodes (such as Au NPs/CPE [7], Au-Pd-RGO/GCE [17], CTAB-Gr-Pt/GCE [44], GO/AgNPs-MIPs/GCE [45] and PDDA-Gr-Pd/GCE [47] in terms of the cost and electrode fabrication.

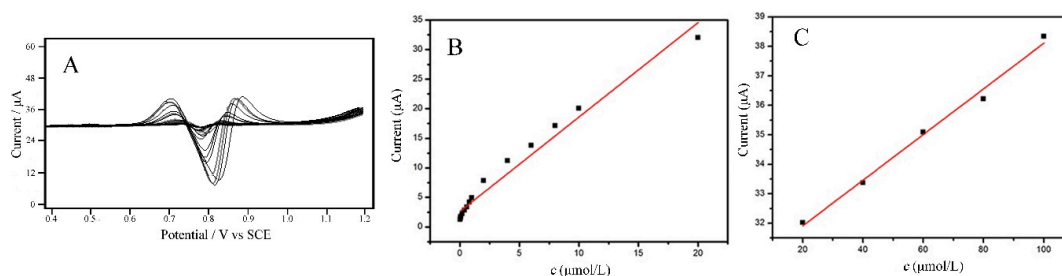


**Figure 8.** (A) Second-derivative linear sweep voltammograms of sunset yellow with various concentrations on the Cu<sub>2</sub>O-ErGO/GCE; Calibration curves between the anodic peak current and the concentrations of sunset yellow ranging from  $2.0 \times 10^{-8}$  to  $2.0 \times 10^{-5}$  mol/L (B) and from  $2.0 \times 10^{-5}$  to  $1.0 \times 10^{-4}$  mol/L (C).

### 2.7. Interference and Reproducibility Investigation

Prior to the detection of real samples, the anti-interference and reproducibility was also investigated to validate the practicability of the proposed Cu<sub>2</sub>O-ErGO/GCE. The response peak current of pure sunset yellow solution and potential interfering compounds mixture solution were recorded and compared. It is observed that the change of  $i_{pa}$  of 10 μmol/L sunset yellow is less than 5% in the presence of a 100-fold concentration of glucose, benzoic acid, citric acid, Na<sup>+</sup>, K<sup>+</sup>, Fe<sup>3+</sup>, and 10-fold concentration of Tartrazine, quinoline yellow (Figure 9). It is demonstrating that our proposed Cu<sub>2</sub>O-ErGO/GCE exhibits good selectivity toward sunset yellow. The reproducibility of Cu<sub>2</sub>O-ErGO/GCEs were examined by continuous measurement the response peak currents of 10 μmol/L sunset yellow seven times. The result shows that the  $i_{pa}$  remain stable with relative standard deviation (RSD) of 2.78% (Table 2), indicating that the Cu<sub>2</sub>O-ErGO/GCE has good reproducibility.

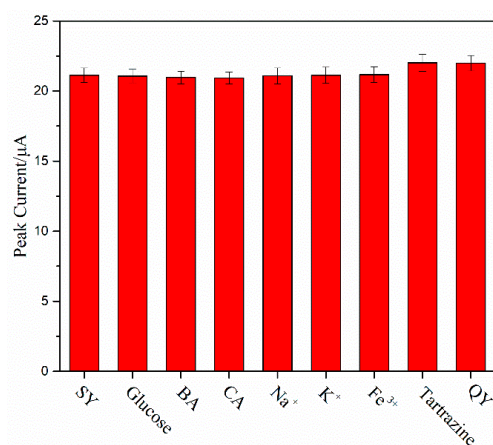


**Figure 9.** The response peak current of Cu<sub>2</sub>O-ErGO/GCE for  $1 \times 10^{-5}$  mol/L sunset yellow (SY) in the presence of interfering substances ( $n = 3$ ). The concentration of glucose, benzoic acid (BA), citric acid (CA), Na<sup>+</sup>, K<sup>+</sup>, Fe<sup>3+</sup>, were  $1 \times 10^{-3}$  mol/L. The concentrations of Tartrazine, quinoline yellow (QY) were  $1 \times 10^{-4}$  mol/L.

**Table 2.** The reproducibility of Cu<sub>2</sub>O-ErGO/GCE for detection of sunset yellow.

No.	1	2	3	4	5	6	7
$i_{pa}$ (µA)	21.07	22.34	21.36	22.04	22.29	22.85	22.24
Average value (µA)				22.02			
RSD (%)				2.78			

### 2.8. Detection Sunset Yellow in Real Samples

Finally, Cu<sub>2</sub>O-ErGO/GCE was applied to determinate sunset yellow in real samples, including carbonated drinks, orange juice, and candy samples. The detect results are listed in Table 3. No anodic peak current is presented in the carbonated beverage sample near 798 mV, indicating that the concentration of sunset yellow is low than the limit of detection. The concentrations of sunset yellow in orange juice and candy samples are detected by 0.085 µmol/L and 0.162 µmol/L, respectively. The content of sunset yellow in these samples is lower than the permitted maximum content that is recommended by national standard (100 µg/mL, namely  $2.2 \times 10^{-4}$  mol/L). Then, an appropriate amount of sunset yellow standard solution was added to the above three samples. Standard addition test results suggests that the recoveries of sunset yellow were 98.75~102.0%, with the relative standard deviation being less than 2.85%, indicating that satisfactory results were obtained using the proposed Cu<sub>2</sub>O-ErGO/GCE. Together with cost-effective, quick response, high sensitive and good selectivity, the Cu<sub>2</sub>O-ErGO/GCE exhibits great prospects on the determination of sunset yellow in different real samples, including but not limiting to beverages, food, and nutrients.

**Table 3.** The results of determination of sunset yellow in soft drink and candies ( $n = 3$ ).

Samples	Original (µmol/L)	Added (µmol/L)	RSD (%)	Found (µmol/L)	Recovery (%)	RSD (%)
Sodas	ND <sup>1</sup>	4	1.28	4.06	102.0	1.50
Orange juice	0.085	0.080	2.46	0.082	102.5	2.31
Candies	0.162	0.160	3.25	0.158	98.75	2.85

<sup>1</sup> ND: Not detected.

## 3. Materials and Methods

### 3.1. Chemical and Solution

Graphite powder, NaNO<sub>3</sub>, concentrated H<sub>2</sub>SO<sub>4</sub>, NaOH, KMnO<sub>4</sub>, H<sub>2</sub>O<sub>2</sub>, CuSO<sub>4</sub>·5H<sub>2</sub>O, Na<sub>2</sub>HPO<sub>4</sub>, NaH<sub>2</sub>PO<sub>4</sub>, hydrochloric acid (HCl), polyvinylpyrrolidone (PVP), hydrate hydrazine (N<sub>2</sub>H<sub>4</sub>·H<sub>2</sub>O), and

ethyl alcohol were analytic grade and supplied by Sinopharm Chemical Reagent Co., Ltd. (Shanghai, China). Sunset yellow was purchased from Aladdin (<http://www.aladdin-e.com>). All of these chemicals were directly used without further purification. A series of sunset yellow standard solutions were prepared by diluting appropriately the stock sunset yellow ( $1 \times 10^{-3}$  mol/L). These standard solutions were kept in 4 °C refrigerator when not in use. Deionized water (18.2 M $\Omega$ ) was used throughout the experiments.

### 3.2. Synthesis of Cu<sub>2</sub>O Nanoparticles

Cu<sub>2</sub>O nanoparticles were synthesized by the hydrothermal method referred to our previous work [18]. Specifically, 50 mg of CuSO<sub>4</sub>·5H<sub>2</sub>O and 24 mg of PVP were added into 10 mL deionized water and then stirred with ultrasonication for 30 min. Afterwards, 2 mL of 0.2 mol/L NaOH solution was added and stirred for 30 min at room temperature to obtain blue Cu(OH)<sub>2</sub> precipitates. Subsequently, 6  $\mu$ L of N<sub>2</sub>H<sub>4</sub>·H<sub>2</sub>O was added as reductant and then stirred for 20 min at room temperature to form a brick red suspension. The precipitate was separated by centrifugation at 5000 rpm, and washed repeatedly with deionized water and ethanol for three times, and vacuum-dried at 60 °C to obtain Cu<sub>2</sub>O nanoparticles.

### 3.3. Preparation Cu<sub>2</sub>O-GO Nanocomposite Dispersion

Graphene oxide (GO) is prepared from cheap graphite powder by a modified Hummers method according to our previous reports [18,19,21]. The as-prepared GO was dispersed in 100 mL of deionized water under ultrasonication for 2 h, and then centrifuged twice to obtain a golden yellow GO solution (1 mg/mL). 2 mg of Cu<sub>2</sub>O nanoparticles were added to 5 mL of the above GO solution, and then ultrasonically dispersed for 2 h to obtain a Cu<sub>2</sub>O-GO nanocomposite dispersion.

### 3.4. Preparation of Cu<sub>2</sub>O-ErGO/GCE

The glassy carbon electrode (GCE,  $\phi = 3$  mm) was polished to a form mirror-like surface with 0.05  $\mu$ m alumina slurry. Then, the electrode was rinsed by deionized water and ethanol alternately (each for 1 min), and then dried by ultrapure N<sub>2</sub> gas. Firstly, 5  $\mu$ L of Cu<sub>2</sub>O-GO dispersion were transferred and coated on the surface of the GCE, and then dried under an infrared lamp to obtain Cu<sub>2</sub>O-graphene oxide nanocomposite modified glass carbon electrode (Cu<sub>2</sub>O-GO/GCE). Then, the GO component was electrochemically reduced by potentiostatic method. Specially, the Cu<sub>2</sub>O-GO/GCE was immersed into 0.1 mol/L PBS solution, and electrochemically reduced at  $-1.2$  V for 120 s. For comparison, GO modified glass carbon electrode (GO/GCE), electrochemically reduced graphene oxide modified glass carbon electrode (ErGO/GCE) and Cu<sub>2</sub>O-GO nanocomposite modified glass carbon electrode (Cu<sub>2</sub>O-GO/GCE) were also fabricated by a similar method.

### 3.5. Electrochemical Measurements

All of the electrochemical measurements were carried out using a standard three-electrode assemble, comprising of bare or modified electrodes as working electrode, saturated calomel electrode (SCE) as reference electrode, and platinum wire electrode as counter electrode. 0.1 M PBS solution was used as supporting electrolytes in all electrochemical experiments. The electrochemical performances of  $1 \times 10^{-5}$  mol/L sunset yellow on various modified electrodes were investigated by cyclic voltammetry (CV) and second-derivative linear sweep voltammetry (SDLSV), with the potential scanning range of 0.4 ~1.2 V. Prior to all electrochemical measurements, an accumulation was performed under stirring at 500 rpm to improve the sensitivity. After 5 s rest, the CV or SDLSV were recorded at a scan rate of 100 mV/s, except where stated otherwise. All of the electrochemical tests were carried on the electrochemical workstation (CHI 760E, Shanghai Chenhua Inc., Shanghai, China).

### 3.6. Analysis of Real Samples

Carbonated drinks, orange juice, and candy samples were purchased from a local supermarket. The same amount of candies was taken out from five packages and carefully grounded into fine powder. Then, the candies powder (about 1.0 g) was accurately weighed and dispersed in 10 mL deionized water under sonication for 1 h. Subsequently, the mixture was centrifuged at 4000 rpm for 10 min to remove insoluble substances. The 0.5 mL as-obtained supernatant was diluted to 10 mL with 0.1 mol/L PBS solution. The liquid samples (carbonated drinks and orange juice) were added into beaker and ultrasonicated for degasification. Then, 1.0 mL of the liquid samples was diluted to 10 mL with 0.1 mol/L PBS solution. Prior to electrochemical detection, accumulation step was performed in the sample solution to enhance the electrochemical response. Then, these sample solutions were detected by second-derivative linear sweep voltammetry while using our proposed Cu<sub>2</sub>O-ErGO/GCE. After each test, Cu<sub>2</sub>O-ErGO/GCE was scanned by cyclic voltammetry a 0.1 mol/L blank PBS solution for several cycles to remove any adsorbents. The modified electrode can be reused only when the response peak disappeared in the blank PBS solution.

## 4. Conclusions

In this study, a promising electrochemical sensor based on the Cu<sub>2</sub>O-ErGO/GCE was developed toward sensing sunset yellow. The Cu<sub>2</sub>O-ErGO nanocomposites not only possess the advantages from individual component materials, but also exhibit obvious synergistic enhancement effects toward sunset yellow. The anodic peak current of sunset yellow on the Cu<sub>2</sub>O-ErGO/GCE increases by about 25 times as compared to that on the bare GCE. The proposed Cu<sub>2</sub>O-ErGO/GCE exhibits two linear regions, namely  $2.0 \times 10^{-8}$  mol/L– $2.0 \times 10^{-5}$  mol/L and  $2.0 \times 10^{-5}$  mol/L– $1.0 \times 10^{-4}$  mol/L, and the limit of detection is  $6.0 \times 10^{-9}$  mol/L (S/N = 3). The sensing performances in terms of linear response ranges and detection limit are comparable to, and even exceed the most reported modified electrodes, such as precious metal-based modified electrodes. Obviously, the Cu<sub>2</sub>O-ErGO/GCE have outstanding advantages over precious metal-based modified electrodes in terms of the cost. Moreover, the response current is basically not affected by potential interfering compounds, suggesting the Cu<sub>2</sub>O-ErGO shows good selectivity. Besides, the good reproducibility was also obtained on the Cu<sub>2</sub>O-ErGO/GCE. Finally, Cu<sub>2</sub>O-ErGO/GCE have been successfully used for the quantitative detection of sunset yellow in real samples (i.e., carbonated beverage, orange juice, and candies) while using second-derivative linear sweep voltammetry. The satisfactory results are obtained with recovery rate is 98.75 ~102.5% and RSD is less than 2.85%. When compared with conventional analytical techniques (Table 4), the proposed method does not require expensive equipment, and time-consuming and complicated pretreatment procedures. Considering the considerable merits including low cost, rapid response, high sensitivity, as well as good selectivity and good reproducibility, the Cu<sub>2</sub>O-ErGO/GCE will have broad application prospects in the detection of sunset yellow in diverse beverages, foods, and nutrients.

**Table 4.** Advantages and drawbacks of previous reported protocols and our proposed protocol.

Protocols	Advantages	Drawbacks
Liquid chromatography	Reliable; good repeatability; high sensitivity; low LOD	Limited separation ability; Time-consuming; expensive equipment
Thin layer chromatography	Low cost apparatus	Organic solvents are often used; they have intensive disagreeable smell and cancerogenic activity
Spectrophotometry	Simultaneous identification and quantification; simple technique	Low sensitivity; extraction separation is needed for detection of dyes in complex product composition
Capillary electrophoresis	High column efficiency, short analysis time and minimal amounts of samples	Limited sensitivity & selectivity; severe matrix interferences
Electrochemical analysis (This work)	Low cost, rapid response, facile operate, high sensitivity and good selectivity	Portability needs to be improved; not disposable

**Author Contributions:** Q.H., G.L. and D.C. conceived and designed the experiments; J.L., X.L., and Y.X. performed the experiments; G.L., P.D., and X.L. analyzed the data; Q.H., J.L. and G.L. wrote the manuscript; Q.H. and D.C. contributed reagents and materials; All authors read and approved the final manuscript.

**Funding:** This research was funded by the NSFC (61703152), Hunan Provincial Natural Science Foundation (2016JJ4010, 2018JJ3134), Project of Science and Technology Department of Hunan Province (GD16K02), Project of Science and Technology Plan in Zhuzhou (201706-201806), Opening Project of Key Discipline of Materials Science in Guangdong (CNXY2017001, CNXY2017002 and CNXY2017003) and the key Project of Department of Education of Guangdong Province (2016GCZX008).

**Conflicts of Interest:** The authors declare no conflict of interest.

## References

1. Ni, Y.; Wang, Y.; Kokot, S. Simultaneous kinetic spectrophotometric analysis of five synthetic food colorants with the aid of chemometrics. *Talanta* **2009**, *78*, 432–441. [[CrossRef](#)] [[PubMed](#)]
2. Al-Degs, Y.S. Determination of three dyes in commercial soft drinks using HLA/GO and liquid chromatography. *Food Chem.* **2009**, *117*, 485–490. [[CrossRef](#)]
3. Mao, Y.; Fan, Q.; Li, J.; Yu, L.; Qu, L. A novel and green ctab-functionalized graphene nanosheets electrochemical sensor for Sudan I determination. *Sens. Actuators B Chem.* **2014**, *203*, 759–765. [[CrossRef](#)]
4. Chung, K.-T.; Cerniglia, C.E. Mutagenicity of azo dyes: Structure-activity relationships. *Mutat. Res.* **1992**, *277*, 201–220. [[CrossRef](#)]
5. Aguilar, F.; Charrondiere, U.R.; Dusemund, B.; Galtier, P.; Gilbert, J.; Gott, D.M.; Grilli, S.; Guertler, R.; Koenig, J.; Lambre, C.; et al. Scientific Opinion on the re-evaluation of Sunset Yellow FCF (E 110) as a food additive on request from the European Commission. *EFSA J.* **2009**, *7*, 1–44.
6. Ye, X.; Du, Y.; Lu, D.; Wang, C. Fabrication of  $\beta$ -cyclodextrin-coated poly (diallyldimethylammonium chloride)-functionalized graphene composite film modified glassy carbon-rotating disk electrode and its application for simultaneous electrochemical determination colorants of sunset yellow and tartrazine. *Anal. Chim. Acta* **2013**, *779*, 22–34. [[PubMed](#)]
7. Ghoreishi, S.M.; Behpour, M.; Golestaneh, M. Simultaneous determination of Sunset yellow and Tartrazine in soft drinks using gold nanoparticles carbon paste electrode. *Food Chem.* **2012**, *132*, 637–641. [[CrossRef](#)] [[PubMed](#)]
8. Minioti, K.S.; Sakellariou, C.F.; Thomaidis, N.S. Determination of 13 synthetic food colorants in water-soluble foods by reversed-phase high-performance liquid chromatography coupled with diode-array detector. *Anal. Chim. Acta* **2007**, *583*, 103–110. [[CrossRef](#)] [[PubMed](#)]
9. Soponar, F.; Cătălin Moț, A.; Sârbu, C. Quantitative determination of some food dyes using digital processing of images obtained by thin-layer chromatography. *J. Chromatogr.* **2008**, *1188*, 295–300. [[CrossRef](#)] [[PubMed](#)]
10. De León-Rodríguez, L.M.; Basuil-Tobias, D.A. Testing the possibility of using UV-vis spectrophotometric techniques to determine non-absorbing analytes by inclusion complex competition in cyclodextrins. *Anal. Chim. Acta* **2005**, *543*, 282–290. [[CrossRef](#)]
11. Yuan, Y.; Zhao, X.; Qiao, M.; Zhu, J.; Liu, S.; Yang, J.; Hu, X. Determination of sunset yellow in soft drinks based on fluorescence quenching of carbon dots. *Spectrochim. Acta A* **2016**, *167*, 106–110. [[CrossRef](#)] [[PubMed](#)]
12. Ryvolová, M.; Táborský, P.; Vrábel, P.; Krásenský, P.; Preisler, J. Sensitive determination of erythrosine and other red food colorants using capillary electrophoresis with laser-induced fluorescence detection. *J. Chromatogr.* **2007**, *1141*, 206–211. [[CrossRef](#)] [[PubMed](#)]
13. Wang, M.; Zhao, J. Facile synthesis of Au supported on ionic liquid functionalized reduced graphene oxide for simultaneous determination of Sunset yellow and Tartrazine in drinks. *Sens. Actuators B Chem.* **2015**, *216*, 578–585. [[CrossRef](#)]
14. Rovina, K.; Siddiquee, S.; Shaarani, S.M. Highly sensitive electrochemical determination of sunset yellow in commercial food products based on CHIT/GO/MWCNTs/AuNPs/GCE. *Food Control* **2017**, *82*, 66–73. [[CrossRef](#)]
15. Wang, J.; Yang, B.; Wang, H.; Yang, P.; Du, Y. Highly sensitive electrochemical determination of Sunset Yellow based on gold nanoparticles/graphene electrode. *Anal. Chim. Acta* **2015**, *893*, 41–48. [[CrossRef](#)] [[PubMed](#)]
16. Thirumalraj, B.; Rajkumar, C.; Chen, S.M.; Veerakumar, P.; Perumal, P.; Liu, S.B. Carbon aerogel supported palladium-ruthenium nanoparticles for electrochemical sensing and catalytic reduction of food dye. *Sens. Actuators B Chem.* **2018**, *257*, 48–59. [[CrossRef](#)]

17. Wang, J.; Yang, B.; Zhang, K.; Bin, D.; Shiraishi, Y.; Yang, P.; Du, Y. Highly sensitive electrochemical determination of Sunset Yellow based on the ultrafine Au-Pd and reduced graphene oxide nanocomposites. *J. Colloid Interface Sci.* **2016**, *481*, 229–235. [[CrossRef](#)] [[PubMed](#)]
18. He, Q.; Liu, J.; Liu, X.; Li, G.; Deng, P.; Liang, J. Preparation of Cu<sub>2</sub>O-reduced graphene nanocomposite modified electrodes towards ultrasensitive dopamine detection. *Sensors* **2018**, *18*, 199. [[CrossRef](#)] [[PubMed](#)]
19. He, Q.; Liu, J.; Liu, X.; Li, G.; Chen, D.; Deng, P.; Liang, J. Fabrication of amine-modified magnetite-electrochemically reduced graphene oxide nanocomposite modified glassy carbon electrode for sensitive dopamine determination. *Nanomaterials* **2018**, *8*, 194. [[CrossRef](#)] [[PubMed](#)]
20. He, Q.; Li, G.; Liu, X.; Liu, J.; Deng, P.; Chen, D. Morphologically tunable MnO<sub>2</sub> nanoparticles fabrication, modelling and their influences on electrochemical sensing performance toward dopamine. *Catalysts* **2018**, *8*, 323. [[CrossRef](#)]
21. He, Q.; Liu, J.; Liu, X.; Li, G.; Deng, P.; Liang, J.; Chen, D. Sensitive and selective detection of Tartrazine based on TiO<sub>2</sub>-electrochemically reduced graphene oxide composite-modified electrodes. *Sensors* **2018**, *18*, 1911. [[CrossRef](#)] [[PubMed](#)]
22. Chen, K.; Wang, M.; Li, G.; He, Q.; Liu, J.; Li, F. Spherical  $\alpha$ -MnO<sub>2</sub> supported on N-KB as efficient electrocatalyst for oxygen reduction in Al–Air battery. *Materials* **2018**, *11*, 601. [[CrossRef](#)] [[PubMed](#)]
23. Wang, M.; Chen, K.; Liu, J.; He, Q.; Li, G.; Li, F. Efficiently enhancing electrocatalytic activity of  $\alpha$ -MnO<sub>2</sub> nanorods/N-doped ketjenblack carbon for oxygen reduction reaction and oxygen evolution reaction using facile regulated hydrothermal treatment. *Catalysts* **2018**, *8*, 138. [[CrossRef](#)]
24. Dorraji, P.S.; Jalali, F. Electrochemical fabrication of a novel ZnO/cysteic acid nanocomposite modified electrode and its application to simultaneous determination of sunset yellow and tartrazine. *Food Chem.* **2017**, *227*, 73–77. [[CrossRef](#)] [[PubMed](#)]
25. Gan, T.; Sun, J.; Meng, W.; Song, L.; Zhang, Y. Electrochemical sensor based on graphene and mesoporous TiO<sub>2</sub> for the simultaneous determination of trace colourants in food. *Food Chem.* **2013**, *141*, 3731–3737. [[CrossRef](#)] [[PubMed](#)]
26. Wu, X.; Zhang, X.; Zhao, C.; Qian, X. One-pot hydrothermal synthesis of ZnO/RGO/ZnO@Zn sensor for sunset yellow in soft drinks. *Talanta* **2018**, *179*, 836–844. [[CrossRef](#)] [[PubMed](#)]
27. Hara, M.; Kondo, T.; Komoda, M.; Ikeda, S.; Kondo, J.N.; Domen, K.; Hara, M.; Shinohara, K.; Tanaka, A. Cu<sub>2</sub>O as a photocatalyst for overall water splitting under visible light irradiation. *Chem. Commun.* **1998**, *3*, 357–358. [[CrossRef](#)]
28. Shao, F.; Sun, J.; Gao, L.; Luo, J.; Liu, Y.; Yang, S. High Efficiency Semiconductor-liquid junction solar cells based on Cu/Cu<sub>2</sub>O. *Adv. Funct. Mater.* **2012**, *22*, 3907–3913. [[CrossRef](#)]
29. Meng, H.; Yang, W.; Ding, K.; Feng, L.; Guan, Y. Cu<sub>2</sub>O nanorods modified by reduced graphene oxide for NH<sub>3</sub> sensing at room temperature. *J. Mater. Chem. A* **2014**, *3*, 1174–1181. [[CrossRef](#)]
30. Wang, Y.; Ji, Z.; Shen, X.; Zhu, G.; Wang, J.; Yue, X. Facile growth of Cu<sub>2</sub>O hollow cubes on reduced graphene oxide with remarkable electrocatalytic performance for non-enzymatic glucose detection. *New J. Chem.* **2017**, *41*, 9223–9229. [[CrossRef](#)]
31. Wang, A.; Li, X.; Zhao, Y.; Wei, W.; Chen, J.; Hong, M. Preparation and characterizations of Cu<sub>2</sub>O/reduced graphene oxide nanocomposites with high photo-catalytic performances. *Powder Technol.* **2014**, *261*, 42–48. [[CrossRef](#)]
32. Tran, P.D.; Batabyal, S.K.; Pramana, S.S.; Barber, J.; Wong, L.H.; Loo, S.C. A cuprous oxide-reduced graphene oxide (Cu<sub>2</sub>O-rGO) composite photocatalyst for hydrogen generation: employing rGO as an electron acceptor to enhance the photocatalytic activity and stability of Cu<sub>2</sub>O. *Nanoscale* **2012**, *4*, 3875–3878. [[CrossRef](#)] [[PubMed](#)]
33. Xie, H.; Duan, K.; Xue, M.; Du, Y.; Wang, C. Photoelectrocatalytic analysis and electrocatalytic determination of hydroquinone by using a Cu<sub>2</sub>O-reduced graphene oxide nanocomposite modified rotating ring-disk electrode. *Analyst* **2016**, *141*, 4772–4781. [[CrossRef](#)] [[PubMed](#)]
34. Li, J.; Wang, X.; Duan, H.; Wang, Y.; Bu, Y.; Luo, C. Based on magnetic graphene oxide highly sensitive and selective imprinted sensor for determination of sunset yellow. *Talanta* **2016**, *147*, 169–176. [[CrossRef](#)] [[PubMed](#)]
35. Deng, K.; Li, C.; Li, X.; Huang, H. Simultaneous detection of sunset yellow and tartrazine using the nanohybrid of gold nanorods decorated graphene oxide. *J. Electroanal. Chem.* **2016**, *780*, 296–302. [[CrossRef](#)]

36. Jampasa, S.; Siangproh, W.; Duangmal, K.; Chailapakul, O. Electrochemically reduced graphene oxide-modified screen-printed carbon electrodes for a simple and highly sensitive electrochemical detection of synthetic colorants in beverages. *Talanta* **2016**, *160*, 113–124. [[CrossRef](#)] [[PubMed](#)]
37. Tkalya, E.E.; Ghislandi, M.; With, G.D.; Koning, C.E. The use of surfactants for dispersing carbon nanotubes and graphene to make conductive nanocomposites. *Curr. Opin. Colloid Interface Sci.* **2012**, *17*, 225–232. [[CrossRef](#)]
38. Songyang, Y.; Yang, X.; Xie, S.; Hao, H.; Song, J. Highly-sensitive and rapid determination of sunset yellow using functionalized montmorillonite-modified electrode. *Food Chem.* **2015**, *173*, 640–644. [[CrossRef](#)] [[PubMed](#)]
39. Qiu, X.; Lu, L.; Leng, J.; Yu, Y.; Wang, W.; Jiang, M.; Bai, L. An enhanced electrochemical platform based on graphene oxide and multi-walled carbon nanotubes nanocomposite for sensitive determination of Sunset Yellow and Tartrazine. *Food Chem.* **2016**, *190*, 889–895. [[CrossRef](#)] [[PubMed](#)]
40. Laviron, E. General expression of the linear potential sweep voltammogram in the case of diffusionless electrochemical systems. *J. Electroanal. Chem.* **1979**, *101*, 19–28. [[CrossRef](#)]
41. Vladislavić, N.; Buzuk, M.; Rončević, I.Š.; Brinić, S. Electroanalytical Methods for Sunset Yellow Determination—A Review. *Int. J. Electrochem. Sci.* **2018**, *13*, 7008–7019. [[CrossRef](#)]
42. Chao, M.; Ma, X. Convenient electrochemical determination of sunset yellow and tartrazine in food samples using a poly(L-phenylalanine)-modified glassy carbon electrode. *Food Anal. Method* **2015**, *8*, 130–138. [[CrossRef](#)]
43. Arvand, M.; Zamani, M.; Sayyar Ardaki, M. Rapid electrochemical synthesis of molecularly imprinted polymers on functionalized multi-walled carbon nanotubes for selective recognition of sunset yellow in food samples. *Sens. Actuators B Chem.* **2017**, *243*, 927–939. [[CrossRef](#)]
44. Yu, L.; Shi, M.; Yue, X.; Qu, L. A novel and sensitive hexadecyltrimethyl ammonium bromide functionalized graphene supported platinum nanoparticles composite modified glassy carbon electrode for determination of sunset yellow in soft drinks. *Sens. Actuators B Chem.* **2015**, *209*, 1–8. [[CrossRef](#)]
45. Qin, C.; Guo, W.; Liu, Y.; Liu, Z.; Qiu, J.; Peng, J. A novel electrochemical sensor based on graphene oxide decorated with silver nanoparticles–molecular imprinted polymers for determination of sunset yellow in soft drinks. *Food Anal. Method* **2017**, *10*, 1–9. [[CrossRef](#)]
46. Sierra-Rosales, P.; Toledo-Neira, C.; Squella, J.A. Electrochemical determination of food colorants in soft drinks using MWCNT-modified GCEs. *Sens. Actuators B Chem.* **2017**, *240*, 1257–1264. [[CrossRef](#)]
47. Yu, L.; Zheng, H.; Shi, M.; Jing, S.; Qu, L. A novel electrochemical sensor based on poly (diallyldimethylammonium chloride)-dispersed graphene supported palladium nanoparticles for simultaneous determination of sunset yellow and tartrazine in soft drinks. *Food Anal. Method* **2016**, *10*, 1–10. [[CrossRef](#)]
48. Arvand, M.; Erfanifar, Z.; Ardaki, M.S. A new core@shell silica-coated magnetic molecular imprinted nanoparticles for selective detection of sunset yellow in food samples. *Food Anal. Method* **2017**, *10*, 1–14. [[CrossRef](#)]

**Sample Availability:** Samples of the compounds are not available from the authors.



© 2018 by the authors. Licensee MDPI, Basel, Switzerland. This article is an open access article distributed under the terms and conditions of the Creative Commons Attribution (CC BY) license (<http://creativecommons.org/licenses/by/4.0/>).